Quantum Transition State Theory for the Collinear $H + H_2$ Reaction

Jie-Lou Liao and Eli Pollak*

Chemical Physics Department, Weizmann Institute of Science, Rehovot, 76100, Israel

Received: October 31, 1999; In Final Form: December 9, 1999

The recently formulated quantum transition state theory (QTST) in which the quantum projection operator is approximated by its parabolic barrier limit and the symmetrized thermal flux is evaluated numerically exactly, is applied to the collinear hydrogen exchange reaction. The results are found to bound the exact results from above for temperatures ranging from $T = 200$ K to $T = 1000$ K. The QTST rate is almost exact at high temperature and is a factor of 3.7 greater than the exact rate at $T = 200$ K, where there is extensive tunneling. Contour plots of the quantum transition state theory reactive flux reveal that the theory accounts well for the "corner cutting" observed in the collinear hydrogen exchange reaction at low temperatures. These results demonstrate that one may estimate quantum rates of bimolecular reactions, using only thermodynamic information.

I. Introduction

Almost thirty years have passed since the first publication of numerically exact quantum rates for the collinear hydrogen exchange reaction.[1] Many articles have been published on approximate theories for this benchmark model (see for example refs 2−5). Why then is it still justified to publish yet another paper, when presumably, this model system is well understood? The collinear hydrogen exchange reaction is arguably the most severe test for a quantum transition state theory. Simple vibrationally adiabatic theories fail[2] due to the rapid change of curvature of the ground-state adiabatic potential in the vicinity of the saddle point. It is only through the use of tailor-made tunneling paths,[6] whose generality is doubtful and whose accuracy is uncontrollable,[7] that good agreement has been obtained between an approximate theory[5] and numerically exact results.

This state of affairs should be contrasted with classical transition state theory[4,7] which is a well-defined theory. It is guaranteed to give an upper bound to the rate. Most approximate quantum theories are usually greater than the exact rate at high temperature but lower at low temperature. Although quantum rate expressions that do bound the exact rate exist,[8−12] they are especially poor in the tunneling regime where they typically go as the square root of the tunneling probability. This state of affairs has almost convinced the community that the search for a quantum transition state theory is doomed to failure.[13]

The past decade has seen though a revival of interest in the formulation of a thermodynamic theory of rates which would be applicable to condensed phase systems.[14] One recent development has been made by Gillan[15] and Voth and coworkers[16−18] who use the quantum centroid density to formulate a thermodynamic rate theory. To the best of our knowledge, the centroid method has yet to be tested on the collinear hydrogen exchange reaction. A different thermodynamic approach has been suggested by Hansen and Andersen,[19] who extrapolate short time thermodynamic coefficients of the flux−flux correlation function[20] to long times. This approach has recently been tested successfully on the $(J = 0)$ 3D $D+H_2$ reaction by Thompson,[21] but only for temperatures greater than $T = 300$ K, where tunneling is not very important.

We have formulated and developed yet a different theory which is based on the Miller−Schwartz−Tromp flux side correlation function expression for the exact quantum rate[20] *k(T)* at temperature T:

$$k(T) = Q_R^{-1} Tr(\hat{F}(\beta, q_{ds})\hat{P}) \tag{1.1}$$

where Q_R is the partition function of reactants, $\hat{H}$ is the Hamiltonian operator, and the symmetrized thermal flux operator $\hat{F}(\beta, q_{ds})$ is defined as

$$\hat{F}(\beta, q_{ds}) = e^{-\beta\hat{H}/2}\hat{F}(q_{ds})e^{-\beta\hat{H}/2} \tag{1.2}$$

$$\hat{F}(q_{ds}) = \frac{1}{2m}[\delta(\hat{q} - q_{ds})\hat{p} + \hat{p}\delta(\hat{q} - q_{ds})] \tag{1.3}$$

$\hat{q}$ and $\hat{p}$ denote the reaction coordinate position and conjugate momentum operators and q_{ds} is the position of an arbitrary dividing surface. The projection operator $\hat{P}$ in eq 1.1 is the long time limit of the time-evolved Heaviside function

$$\hat{P} = \lim_{t=\infty} e^{i\hat{H}t/\hbar}\hat{h}(\hat{q})e^{-i\hat{H}t/\hbar} \tag{1.4}$$

Quantum transition state theory (referred to as QTST throughout the rest of this paper) is derived[22,23] by noting that the trace in eq 1.1 can be written exactly as a phase space integral over the Wigner phase space representations of the two operators, $\hat{P}$ and $\hat{F}$ (β, q_{ds}). The symmetrized thermal flux operator in phase space is calculated using Monte Carlo methods while, as suggested by Voth et al.,[24] the exact projection operator is replaced by its parabolic barrier limit. The accuracy of QTST has been thus far tested for symmetric[22] and asymmetric[23] one-dimensional Eckart barriers, and for a model two-dimensional system in which a harmonic oscillator is bilinearly coupled to a symmetric Eckart barrier in ref 25. In all cases studied thus far QTST bounded the exact quantum rate from above and was within factors of 2−3 of the exact rate even for tunneling factors of 10^3.

* Corresponding author.

10.1021/jp993865b CCC: $19.00
Published on Web 02/15/2000

QTST can be systematically improved.[23] Because of the approximate harmonic projection operator, the QTST expression for the rate depends on the location of the dividing surface. Varying the location and choosing the minimal flux leads to significant improvement of the rate estimate in asymmetric systems.[23] Moreover, the parabolic barrier expression for the projection operator is just the leading term in an expansion of the exact projection operator in terms of the nonlinear part of the potential. Adding in the leading order correction term gives a systematic improvement for the rate estimate.[23] A semiclassical study of variational QTST has also been presented in ref 26.

The purpose of this paper is to apply QTST to the $H + H_2$ system. We shall provide a comparison between QTST and the numerically exact results of Bondi et al.[5] based on the LSTH potential energy surface.[27−29] We find that QTST bounds the exact rate from above for all temperatures studied. At low temperatures ($T = 200$ K) QTST gives an estimate which is a factor of 3.7 greater than the exact rate. It becomes increasingly accurate as the temperature is increased. These results present a significant improvement over previous work in which the dividing surface was chosen to be the planar symmetric stretch surface. Perhaps not less interesting is the structure of the QTST reactive flux in the configuration space. At low temperatures one finds extensive "corner cutting"[3] and the flux oscillates between positive and negative values that almost cancel each other out. As the temperature is increased, the flux becomes more localized in the saddle point region and is positive almost everywhere.

The arrangement of this paper is as follows. The QTST formalism for systems with two degrees of freedom is reviewed and applied to the collinear $H + H_2$ system in Section II. Numerical results are presented in Section III. We end in Section IV with a discussion on the implications of these results for future applications to 3D H+H_2 and its isotopic derivatives, as well as larger systems.

II. QTST for the Collinear $H + H_2$ System

A. QTST for Systems with Two Degrees of Freedom. The Hamiltonian of the system is assumed to take the form

$$H = \frac{1}{2}(p_q^2 + p_y^2 - w^{\ddagger 2}q^2 + w_y^2 y^2) + V_1(q, y) \qquad (2.1)$$

where q is the (mass weighted) unstable normal mode at the saddle point of the potential energy surface and y is the stable mode. Without loss of generality, the saddle point is assumed to be located at $q = y = 0$. p_q, p_y are the momenta conjugate to q, y, respectively, and $w^{\ddagger}$, w_y are the harmonic frequencies of the normal modes at the saddle point.

With these preliminaries, the exact rate expression may be written as

$$k(T) = Q_R^{-1} \int_{\infty}^{-\infty} dy_{ds} Tr[\hat{F}(\beta, q_{ds} = 0, y_{ds})\hat{P}] \qquad (2.2)$$

where the multidimensional symmetrized quantum thermal flux operator is written as

$$\hat{F}(\beta, q_{ds} = 0, y_{ds}) = e^{-\beta\hat{H}/2}\, \hat{F}(0, y_{ds}) e^{-\beta\hat{H}/2} \qquad (2.3)$$

and $\hat{F}(0, y_{ds})$ is

$$\hat{F}(0, y_{ds}) = \frac{1}{2}\delta(\hat{y} - y_{ds})[\hat{p}_q \delta(\hat{q}) + \delta(\hat{q})\hat{p}_q] \qquad (2.4)$$

QTST implies replacing the exact projection operator with its parabolic barrier approximation. The Wigner representation of the parabolic barrier projection operator is[22,30]

$$P_W^{(pb)}(p, q) = \frac{1}{2\pi\hbar} h(p + w^{\ddagger} q) \qquad (2.5)$$

The QTST rate expression is thus

$$k_{QTST}(T) = \frac{1}{Q_R}\int_{-\infty}^{\infty} dp \int_{-\infty}^{\infty} dq h(p + w^{\ddagger} q) F_W((\beta, q_{ds} = 0); p, q) \qquad (2.6)$$

where the (reduced) Wigner representation of the thermal flux operator in the phase space of the reaction coordinate is

$$\hat{F}_W((\beta, q_{ds} = 0); p, q) = \frac{1}{2\pi\hbar}\int_{-\infty}^{\infty} dy_{ds} \int_{-\infty}^{\infty} dy \int_{-\infty}^{\infty} d\xi\, e^{i\xi p/\hbar} \langle q - \xi/2, y|\hat{F}((\beta, q_{ds} = 0, y_{ds}); q, y)|q + \xi/2, y\rangle \qquad (2.7)$$

The matrix element of the flux operator is[31]

$$\langle q'', y|\hat{F}(\beta, q_{ds} = 0, y_{ds})|q', y\rangle = \frac{i\hbar}{2}\int_{-\infty}^{\infty} dy_{ds} \left[\langle q'', y|e^{-\beta\hat{H}/2}|q_{ds}, y_{ds}\rangle \left\langle \frac{\partial}{\partial q_{ds}}, y_{ds}\middle| e^{-\beta\hat{H}/2}\middle| q', y\right\rangle - \left\langle q'', y\middle| e^{-\beta\hat{H}/2}\middle| \frac{\partial}{\partial q_{ds}}, y_{ds}\right\rangle \langle q_{ds}, y_{ds}|e^{-\beta\hat{H}/2}|q', y\rangle\right]_{q_{ds}=0} \qquad (2.8)$$

where we used the shorthand notation

$$\left\langle q'', y\middle| e^{-\beta\hat{H}/2}\middle| \frac{\partial}{\partial q_{ds}}, y_{ds}\right\rangle \equiv \left[\frac{\partial}{\partial q'}\langle q'', y|e^{-\beta\hat{H}/2}|q', y_{ds}\rangle\right]_{q'=q_{ds}} \qquad (2.9)$$

Using the Fourier expansion of the Heaviside function:

$$h(p + w^{\ddagger} q) = \frac{1}{2\pi i}\int_{-\infty}^{\infty} \frac{dk}{k} e^{ik(p + w^{\ddagger} q)} \qquad (2.10)$$

one may write the QTST estimate for the rate constant as

$$k_{QTST}(T) = Q_R^{-1}\frac{\hbar}{4\pi}\int_{-\infty}^{\infty} dq \int_{-\infty}^{\infty} d\xi \frac{\cos\left(\frac{w^{\ddagger} q\xi}{\hbar}\right)}{\xi} F(q - \xi/2, q + \xi/2) \qquad (2.11)$$

where the symbol $F(q'', q')$ denotes a bath-integrated flux function

$$F(q'', q') = \int_{-\infty}^{\infty} dy \int_{-\infty}^{\infty} dy_{ds} \left[\langle q'', y|e^{-\beta\hat{H}/2}|q_{ds}, y_{ds}\rangle \left\langle \frac{\partial}{\partial q_{ds}}, y_{ds}\middle| e^{-\beta\hat{H}/2}\middle| q', y\right\rangle - \left\langle q'', y\middle| e^{-\beta\hat{H}/2}\middle| \frac{\partial}{\partial q_{ds}}, y_{ds}\right\rangle \langle q_{ds}, y_{ds}|e^{-\beta\hat{H}/2}|q', y\rangle\right] \qquad (2.12)$$

which can be evaluated using the path integral Monte Carlo method. In practice, we used the same harmonic representation of the paths as given in detail in ref 25 to evaluate the imaginary time matrix elements.

B. Specifics for the Collinear H+H_2 Reaction. The LSTH potential surface[27−29] is given in terms of the bond coordinates $R_{H_AH_B}$ and $R_{H_BH_C}$ and collinearity is assured by the relation $R_{H_AH_C} = R_{H_AH_B} + R_{H_BH_C}$. The saddle point is located at $R^{\ddagger}_{H_BH_C}$, $R^{\ddagger}_{H_AH_B}$.

TABLE 1: Saddle Point Parameters of the LSTH Potential Energy Surface

$V^{\ddagger}$(kcal/mol)	9.802
$R^{\ddagger}_{H_BH_C}(a_0)$	1.757
$w^{\ddagger}(\mathrm{cm}^{-1})$	1505
$w_y(\mathrm{cm}^{-1})$	2056

To apply QTST one must transform to the mass weighted normal modes at the saddle point. Because of symmetry these are the symmetric (y) and the antisymmetric (q) stretch coordinates. Denoting the mass of the hydrogen atom as m_H, these may be expressed in terms of the bond coordinates as.[32]

$$q = \sqrt{\frac{m_H}{6}}\,(R_{H_AH_B} - R_{H_BH_C}) \tag{2.13}$$

$$y = \sqrt{\frac{m_H}{2}}\,[(R_{H_AH_B} - R^{\ddagger}_{H_AH_B}) + (R_{H_BH_C} - R^{\ddagger}_{H_BH_C})] \tag{2.14}$$

With these preliminaries the (LSTH) collinear potential energy surface is expressed as

$$V[R_{H_AH_B}(q,y), R_{H_BH_C}(q,y)] \equiv V^{\ddagger} - \frac{1}{2}w^{\ddagger 2}q^2 + \frac{1}{2}w_y^2y^2 + V_1(q,y) \tag{2.15}$$

where $V^{\ddagger}$ is the energy of the saddle point, the frequencies $w^{\ddagger}$, w_y are given by the square root of the second derivatives of the potential with respect to the antisymmetric and symmetric stretch coordinates at the saddle point, respectively, and V_1 is the anharmonic remainder of the full potential. The saddle point energy, location, and harmonic frequencies of the LSTH potential surface are given in Table 1.

III. Numerical Results

Details of the Monte Carlo method have been presented in refs 25, 33. Here we just note that to aid the convergence, especially at low temperatures where $\hbar\beta w^{\ddagger} \geq 2\pi$ we used a suitable harmonic reference potential $V_{ref}(q, y)$ with an antisymmetric stretch frequency which is lower than the true frequency. This just causes a redefinition of the nonlinear part of the potential V_1 which includes the difference between the true saddle point frequencies and the reference ones used.

As shall be shown further on, especially at low temperatures, it is crucial that the configuration space which is sampled is sufficiently large to include the full range of the rather delocalized flux function. The coordinates were sampled in the region $0.95a_0 \leq R_{H_BH_C}, R_{H_AH_B} \leq 3.52a_0$. The maximal order of the harmonic decomposition of the paths we used was 40 for $T = 200$ K and 15 for $T = 1000$ K. A sampling of 10^6 points was taken for $T = 200$ K and 5×10^4 points for $T = 1000$ K. For further computational details see also ref 25.

The reactants partition function is

$$Q_R = \sqrt{\frac{\mu}{2\pi\hbar^2\beta}}\,Q_V \tag{3.1}$$

where $\mu = 2/3\ m_H$ is the translational reduced mass of H_A relative to H_BH_C and Q_V is the vibrational partition function of the (one dimensional) H_2 molecule. The computed values of Q_V are given in Table 2.

The QTST estimates for the collinear rate constants are compared in Table 2, with the numerically exact results of ref 5 and are plotted as an Arrhenius plot in Figure 1. For $T = 1000$ K, QTST overestimates the exact result by ~6% while at $T = 200$ K the overestimate is by a factor of 3.7. The error bars on the computation (estimated from the standard deviation of a few independent runs at the same temperature) are small at high temperatures (1% for $T = 1000$ K) but increase as the temperature is lowered (~20% at $T = 200$ K).

TABLE 2: Rate Constants for the Collinear H + H_2 Reaction on the LSTH Potential Energy Surface[a]

T	Q_V^b	k_{ex}^c	k_{QTST}^d
200	1.54×10^{-7}	6.20×10^{-2}	$(2.3 \pm 0.4) \times 10^{-1}$
300	2.87×10^{-5}	4.81	9.2 ± 0.7
400	3.92×10^{-4}	5.46×10^{1}	$(7.9 \pm 0.2) \times 10^{1}$
600	5.36×10^{-3}	7.26×10^{2}	$(8.3 \pm 0.2) \times 10^{2}$
1000	4.35×10^{-2}	6.68×10^{3}	$(7.1 \pm 0.1) \times 10^{3}$

[a] QTST rate constants (in *cm molecule*$^{-1}$ *s*$^{-1}$) are compared with the numerically exact rates. [b] Q_V are the computed values of the vibrational partition function of the H_2 diatomic molecule as obtained from the LSTH potential energy surface. [c] The numerically exact results are taken from ref 5. [d] Error bars are the standard deviation.

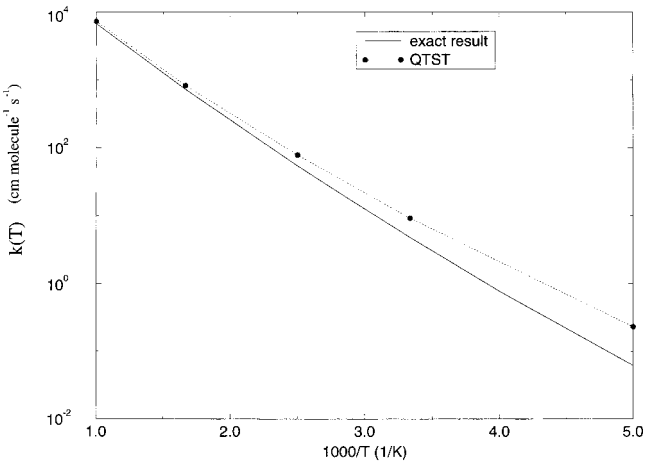

Figure 1. Comparison of QTST with the numerically exact quantum rates for the collinear hydrogen exchange reaction using an Arrhenius plot.

To obtain a deeper understanding for the increasing difficulty in computing the QTST rate at low temperatures we plot the configuration space representation $F(q, y)$ of the QTST flux, defined by

$$k_{QTST}(T) \equiv \frac{1}{Q_R}\int_{-\infty}^{\infty} \mathrm{d}q \int_{-\infty}^{\infty} \mathrm{d}y F(q,y) \tag{3.2}$$

Contour plots of the QTST reactive flux $F(q, y)$ are shown in panels a−c of Figure 2 for $T = 1000$, 400, and 200 K, respectively.

At $T = 1000$ K, the reactive flux distribution is positive and localized in the saddle point region. This is the typical high temperature behavior, found also in our previous studies of the one-dimensional Eckart potential.[23] As the temperature is lowered, the reactive flux becomes increasingly oscillatory and delocalized, with extensive corner cutting at positive values of the symmetric stretch coordinate y. It is the combination of delocalization and oscillatory structure which makes the computation increasingly more difficult. The delocalization implies that a larger region of configuration space must be sampled. But the real difficulty comes from the oscillatory structure. The cancellation of positive and negative flux leads to only a small net reactive flux. The positive and negative parts must be evaluated sufficiently accurately so that the difference between them remains numerically significant.

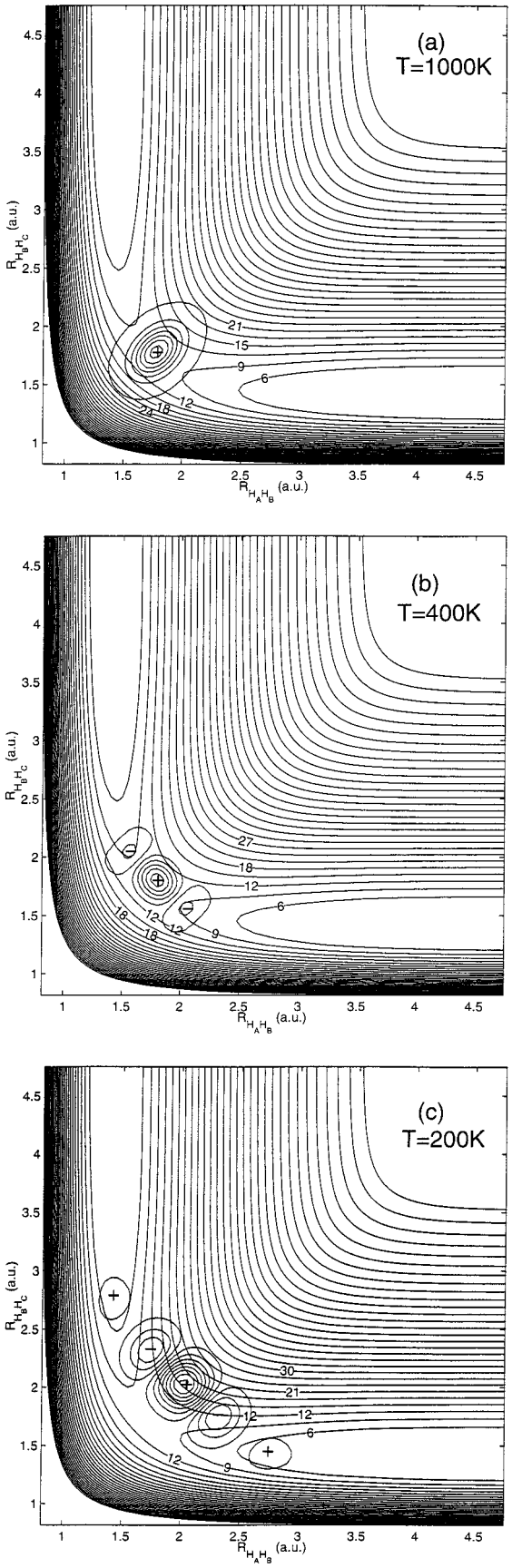

Figure 2. Contour plots of the QTST reactive flux distribution in configuration space. Panels a−c correspond to the temperatures of $T = 1000$, 400, and 200 K, respectively. Contours of the LSTH potential energy surface are given for every 3 kcal/mol, from 6 to 90 kcal/mol.

Interestingly, the QTST accounts well for the corner cutting, even though no special effort was made, such as the use of special tunneling paths. The fact that the thermal flux operator matrix elements are computed numerically exactly suffices for getting the right "physics". The only source of error is in the use of the parabolic barrier projection operator.

IV. Discussion

We have demonstrated that QTST provides a reasonable estimate for the thermal collinear rate constant of the hydrogen exchange reaction. Even though we use the simple parabolic barrier projection operator, QTST does account well for the extensive corner cutting found in this reaction at low temperatures.

In QTST the dividing surface, taken to be the surface perpendicular to the unstable mode at the saddle point is by definition planar. The results of QTST should thus be compared to other transition state theory like approximations in which the same planar dividing surface is used. In fact, all previous planar dividing surface theories gave worse results. Even introduction of curvature to the reaction coordinate such as in the ICVT/MEPSAG prescription[34] gives a result which is a factor of almost 7 smaller than the numerically exact result at $T = 200$ K.[5] Computations on other potential energy surfaces also give results whose quality is worse than QTST.[35] One of the reasons why QTST is superior is that the thermal flux is treated exactly, it includes in it the full Hamiltonian. In contrast to the older prescriptions, there isn't any need to "optimize" the curved coordinate system to include the "correct" dynamical effects. They are automatically included in QTST.

A second noteworthy and nontrivial aspect is that the QTST estimates are found to bound the exact rate from above for all temperatures considered. All other approximate expressions, including ICVT/MCPSAG give results which are sometimes above and sometimes below the true rate. We do not have a rigorous proof that QTST will always bound the rate from above but can rationalize the result. At high temperatures, the thermal flux is positive (for positive momenta) and localized in the vicinity of the dividing surface. Classical recrossings would reflect themselves as structure and delocalization of the projection operator. Therefore at sufficiently high temperatures, QTST bounds the true rate from above.

The only error in QTST is in the parabolic barrier approximation for the projection operator. The exact quantum projection operator in phase space, differs from the parabolic barrier projection operator in two aspects. The nonlinearity of the potential causes the exact classical projection operator to be more delocalized and structured than the parabolic barrier approximation. Thus, at low temperatures, where the thermal flux delocalizes, QTST underestimates the contribution from the negative (delocalized) portion of the flux[23] and so gives an enlarged estimate for the rate. Secondly, the exact projection operator in phase space is not a discontinuous function such as the Heaviside function but as noted in ref 23, resembles the integral of an Airy function. The leading order correction terms resulting from this oscillatory behavior also lead to a reduction of the rate and come from the negative parts of the exact projection operator. Since the negative region is typically distant from the saddle point, it becomes important only when the thermal flux is delocalized, this occurs at low temperatures, as shown in Figure 2.

These observations imply that an improved estimate for the rate could be obtained by replacing the parabolic barrier projection operator with the exact classical projection operator.

The ensuing mixed quantum classical rate theory (MQCLT) indeed does improve the rate estimates as shown for a model system with two degrees of freedom studied in detail in ref 33. MQCLT becomes though exceedingly difficult to apply as the number of degrees of freedom of the system increases, since it involves a determination of the Wigner representation of the symmetrized thermal flux operator in the full phase space. In N dimensions, this calls for an N-dimensional Fourier transform, making a Monte Carlo evaluation almost as difficult as an exact quantum computation.

The present QTST results at low temperatures are not as close to the exact results as the ICVT-MCPSAG results of ref 5. However, the same ICVT-MCPSAG prescription is not foolproof either; for example, it fails at low temperatures for the asymmetric $Mu + D_2$ reaction on the Porter−Karplus potential energy surface.[5,7] The Marcus−Coltrin path is a useful construct but it does not lead to a well-defined thermodynamic rate theory, in the sense that one can evaluate a leading term in an expansion and if necessary also further correction terms. QTST is well defined and we know how to improve it systematically if we so desire. As already mentioned the first step would be obtained by replacing the parabolic barrier projection operator with the classical projection operator.[23,33] A second step would be obtained by including the leading order correction term in the nonlinearity to the parabolic barrier projection operator. A third improvement would be to use a semiclassical initial value representation for the projection operator, as implemented on some model problems by Sun et al. in ref 36.

Perhaps the major disadvantage of QTST, as compared to the ICVT class of prescriptions[34] is that the numerical effort involved in QTST is substantially larger. Numerical computation of the symmetrized thermal flux operator matrix elements does involve path integral Monte Carlo methods which are computationally expensive. But with present day fast computers these are becoming routine and have not yet presented us with a major stumbling block.

The fact that QTST depends only on the saddle point normal modes, means that it is formally easy to generalize it to larger systems. We did not use any sophisticated approximation based for example on the Marcus−Coltrin path or the reaction path. In this sense, QTST mimics classical TST. For example, for the full 3D hydrogen exchange reaction, it would suffice to use the Cartesian representation of the symmetric and antisymmetric stretch coordinates to obtain the QTST estimate for the full thermal rate. The averaging over angular momentum would be automatically built in. Since quantum tunneling effects become smaller as the dimensionality increases, we expect that QTST will lead to more accurate estimates for the rate, even at low temperatures.

In this paper we have applied QTST to the symmetric hydrogen exchange reaction. There is nothing which limits QTST to symmetric systems. In an asymmetric system, one must only find the normal modes at the saddle point. On the basis of our previous studies of one-dimensional asymmetric systems[23] it is to be expected that use of the variational version of QTST will become important as the asymmetry becomes larger. Whether one can then remain with the unstable mode as the location of the dividing surface or whether one would have to resort for example to variation along the minimum energy path, is a topic for future studies.

Acknowledgment. Stimulating discussions with Prof. A. Kuppermann are gratefully acknowledged. This work has been supported by grants from the Minerva Foundation, Munich/Germany, the German Israeli Foundation for Basic Research, the Israel Science Foundation, and the U.S.-Israel Binational Science Foundation.

References and Notes

(1) Truhlar, D. G.; Kuppermann, A. *J. Chem. Phys.* **1970**, *52*, 3841.
(2) Truhlar, D. G.; Kuppermann, A. *Chem. Phys. Lett.* **1971**, *9*, 269.
(3) Chapman, S.; Garrett, B. C.; Miller, W. H. *J. Chem. Phys.* **1975**, *63*, 2710.
(4) Pechukas, P. *Annu. Rev. Phys. Chem.* **1981**, *32*, 159.
(5) Bondi, D. K.; Clary, D. C.; Connor, J. N. L.; Garrett, B. C.; Truhlar, D. G. *J. Chem. Phys.* **1982**, *76*, 4986.
(6) Marcus, R. A.; Coltrin, M. E. *J. Chem. Phys.* **1977**, *67*, 2609.
(7) Pollak, E. In *Theory of Chemical Reaction Dynamics*; Baer, M., Ed.; CRC Press: Boca Raton, F1, 1985; Vol. 3, p 123.
(8) McLafferty, F. J.; Pechukas, P. *Chem. Phys. Lett.* **1974**, *27*, 511.
(9) Pollak, E. *J. Chem. Phys.* **1981**, *74*, 6765.
(10) Pollak, E.; Proselkov, D. *Chem. Phys.* **1993**, *170*, 265.
(11) Muga, J. G.; Delgado, V.; Sala, R.; Snider, R. F. *J. Chem. Phys.* **1996**, *104*, 7015.
(12) Pollak, E. *J. Chem. Phys.* **1997**, *107*, 64.
(13) Miller, W. H. In *Dynamics of Molecules and Chemical Reactions*; Wyatt, R. E.; Zhang, J. Z. H. Eds.; Marcel Dekker Inc.: New York, 1996.
(14) Hänggi, P.; Talkner, P.; Borkovec, M. *Rev. Mod. Phys.* **1990**, *62*, 251.
(15) Gillan, M. J. *J. Phys. C.: Solid State Phys.* **1987**, *20*, 3621.
(16) Voth, G. A.; Chandler, D.; Miller, W. H. *J. Chem. Phys.* **1989**, *91*, 7749.
(17) Voth, G. A. *J. Phys. Chem.* **1993**, *97*, 8365.
(18) Cao, J.; Voth, G. A. *J. Chem. Phys.* **1996**, *105*, 6856.
(19) Hansen, N. F.; Andersen, J. C. *J. Chem. Phys.* **1994**, *101*, 6032.
(20) Miller, W. H.; Schwartz, S. D.; Tromp, J. W. *J. Chem. Phys.* **1983**, *79*, 4889.
(21) Thompson, W. H. *J. Chem. Phys.* **1999**, *110*, 4221.
(22) Pollak, E.; Liao, J.-L. *J. Chem. Phys.* **1998**, *108*, 2733.
(23) Shao, J.; Liao, J.-L.; Pollak, E. *J. Chem. Phys.* **1998**, *108*, 9711.
(24) Voth, G. A.; Chandler, D.; Miller, W. H. *J. Phys. Chem.* **1989**, *93*, 7009.
(25) Liao, J. L.; Pollak, E. *J. Chem. Phys.* **1999**, *109*, 80.
(26) Pollak, E.; Eckhardt, B. *Phys. Rev. E* **1998**, *58*, 5436.
(27) Liu, B. *J. Chem. Phys.* **1973**, *58*, 1925.
(28) Liu, B.; Siegbahn, P. *J. Chem. Phys.* **1978**, *68*, 2457.
(29) Truhlar, D. G.; Horowitz, C. J. *J. Chem. Phys.* **1978**, *68*, 2466; **1979**, *71*, 1514(E).
(30) Georgievskii, Y.; Pollak, E. *J. Chem. Phys.* **1995**, *103*, 8910.
(31) Pollak, E. *J. Chem. Phys.* **1997**, *107*, 64.
(32) Wilson, E. B., Jr.; Decius, J. C.; Cross, P. C. *Molecular Vibrations*; McGraw-Hill: New York, 1955.
(33) Liao, J. L.; Pollak, E. *J. Chem. Phys.* **1999**, *111*, 7244.
(34) Truhlar, D. G.; Isaacson, A. D.; Garrett, B. C. In *Theory of Chemical Reaction Dynamics*; Baer, M. Ed.; CRC Press: Boca Raton, Fl, 1985; Vol. 4, p 65.
(35) Truhlar, D. G.; Kuppermann, A. *J. Chem. Phys.* **1972**, *56*, 2232.
(36) Sun, X.; Wang, H.; Miller, W. H. *J. Chem. Phys*, **1998**, *109*, 4190; ibid, 1998, *109*, 7064.